

Advanced Guidance Law Design for Trajectory-Corrected Rockets with Canards under Single Channel Control

Qing-wei Guo, Wei-dong Song, Min Gao, Dan Fang

Abstract—At present, unguided rockets are the main form of battle ammunition among conventional weapons. They are used as mass-kill weapons because of their power, but they lack precision and can result in significant collateral damage. This paper will demonstrate a new type of trajectory-corrected rocket, controlled by a pair of canards in a single channel. Control is accomplished by canard deflections to generate a directional force and correct the ballistic trajectory. The primary guidance and control mechanisms are presented, along with the rocket trajectory characteristics and canard features. A guidance law for these trajectory-corrected rockets is identified, which consists of separate ascending and descending trajectory guidance laws. An advanced transverse guidance law is applied to the ascending trajectory to fit the trajectory curve and solve the issue of the lack of line-of-sight information. The proportional guidance law used during the descending trajectory also needs to be advanced to fit the large curvature and lack of control authority. The hardware is assessed using a loop simulation to verify the success of the guidance law with a high-fidelity control assembly, comprising a projectile-borne computer, a canard actuator, and guidance law algorithms. In addition, a Monte Carlo analog target simulation is carried out to prove that the algorithms are both feasible and effective..

Index Terms—trajectory-corrected rockets, guidance law design, canard, control in single channel, simulation analysis

I. INTRODUCTION

CONVENTIONAL unguided rockets are still the main form of battle ammunition used today as mass-kill weapons. They provide strong power but poor precision, which leads to significant collateral damage. Modern war requires that a weapon should be low-cost and high-precision, successfully killing point targets without causing much collateral damage. Precision-guided weapons can reach relatively high accuracy, but they are always so expensive that economically underdeveloped countries cannot afford them,

Manuscript received June 29, 2016; revised August 31, 2016. This work is supported by National Natural Science Foundation of China.

Qingwei Guo is currently pursuing the PH.D. degree in Shijiazhuang Mechanical Engineering College, Shijiazhuang 050003, China (corresponding author phone: +86031187994463; e-mail: gqingwei@sina.cn).

Wei-dong Song, is with Shijiazhuang Mechanical Engineering College, Shijiazhuang 050003, China (e-mail: wdsung@163.com).

Min Gao is with Shijiazhuang Mechanical Engineering College, Shijiazhuang 050003, China (e-mail: gaomin1103@yeah.net).

Dan Fang is with Shijiazhuang Mechanical Engineering College, Shijiazhuang 050003, China (e-mail: aq_fd@126.com).

and the high cost even creates a hindrance for developed nations such as the United States [1]-[3]. Trajectory-correction technology could provide a means of reducing the cost while improving the precision of such rockets [4]-[7].

In 1994, during the Gulf War, the American military developed the XM30 Guided Multiple Launch Rocket System (GMLRS), a rocket guidance system with trajectory correction [5], [8]. A guidance kit is mounted to the front of the MLRS, and comprises an Inertial Measurement Unit (IMU), four independent electro-mechanically actuated canards, a Global Positioning System (GPS) receiver, GPS antennas, a thermal battery, a guidance computer, and power supply electronics. Israel Aircraft Industries (IAI) and Israel Military Industries (IMI) have introduced their jointly-developed munitions, the Extended Range Artillery (EXTRA) rockets. An EXTRA rocket includes a GPS/INS unit and the trajectory is corrected by engine thrusts supplied by a gas generator. The German Rheinmetall Defence developed Contraves Rheinmetall Enhanced Correction of Trajectories (CORECT) rockets, with a guidance module consisting of a guidance and control (G&C) unit located inside the ogival front section of the rocket just aft of the nose-mounted fuze. The on-board GPS satellite navigation system receiver determines the actual position of the rocket during flight, allowing the G&C unit to determine the difference between the actual and desired trajectories, and then to calculate the required correction. The probable circular error for the standard rocket is up to 580 m at maximum range, but the CORECT module reduces this to less than 50 m.

In this paper, we propose a new concept of trajectory correction based only on Global Positioning System (GPS) data and geomagnetic measurements, and we present the corresponding guidance law when using a pair of canards in a single channel. The main configuration and the primary G&C mechanisms are demonstrated in Section II. The guidance law is presented specifically in Section III. The results of loop and Monte Carlo simulations are presented in Section IV. Finally, the conclusions are presented in Section V.

II. CONFIGURATION AND G&C MECHANISMS

A. Trajectory-Corrected Rocket Configuration



Fig. 1. Configuration of the trajectory-corrected rocket

As shown in Figure 1, the proposed trajectory-corrected rocket consists of four fins, an engine, a warhead, a fuze, and a G&C system. The G&C system is the key component used in trajectory correction and is described in detail here. It includes a projectile-borne computer, guidance electronics, control assemblies, and guidance law algorithms. The primary purpose of the computer is to receive the GPS data and geomagnetic measurements in order to calculate the appropriate guidance solution, and to use the guidance data and the pre-specified target location to calculate the control commands. The guidance electronics are composed of GPS receivers and geomagnetic sensors, which provide the projectile position, velocity, and attitude. The control assemblies include a pair of canards, which are mounted on the nose of the body, and the actuator, which implements the control commands and generates the canard deflection. In this specific case, the two canards can only rotate about a single axle with the same speed and produce the same deflection [9]-[11]. In addition, a battery is included to supply the system with power.

B. Guidance and Control Mechanisms

Common guidance control mechanisms include pulse thrusters and aerodynamic forces created by changes in the projectile configuration. The canards in a single-channel control mechanism like that employed in this paper are applications of the aerodynamic control force. Using variations in the canard deflection, the lift force can be modified with the deflection angle and the control force is produced.

The G&C mechanism works as follows. Following the launch, the G&C system is powered on and the GPS receivers demonstrate their ability to reacquire the GPS satellite data within approximately 5 seconds. The real-time projectile position and velocity can be obtained from the GPS navigation data. The geomagnetic sensors are initiated and measure the components of the geomagnetic field in the projectile cross-section simultaneously. Attitude estimates can be established by attitude determination algorithms that use the geomagnetic measurement data [12]. The projectile-borne computer combines the GPS navigation data with the geomagnetic measurement data to produce a 100-Hz navigation solution, and utilizes the navigation data with the pre-specified target location to generate the trajectory deviation between the flight path and the desired path. A guidance law must be applied to use the navigation data and the pre-specified target location to resolve the trajectory deviation and to produce the guidance commands. The control commands are computed using the algorithm and are transmitted to the canard actuator, which then executes the canard deflection. From the canard deflection angle and the

expected roll angle, the control roll angle γ_c is determined and a directional control force is provided to reduce the trajectory deviation and to steer the projectile to the desired target. A block diagram of this mechanism is shown in Figure 2.

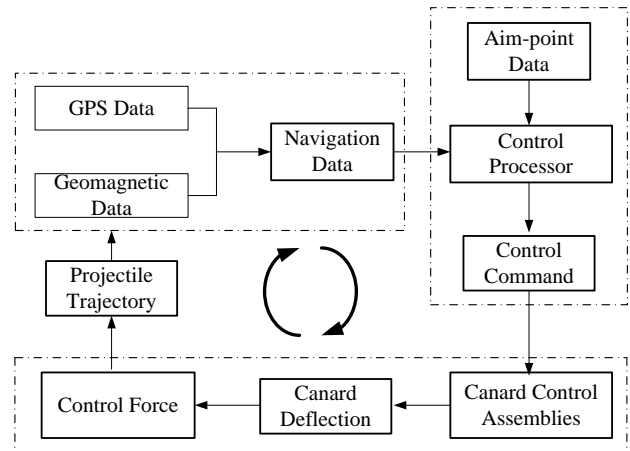


Fig. 2. The G&C mechanism and flow diagram

The program applies the necessary canard deflection to change the projectile aerodynamic configuration and provide the required control force. The control force can be supplied continuously and effectively to correct the trajectory deviation.

III. GUIDANCE LAW DESIGN

A. Problem Formulation

Guidance law design is the critical factor in determining the success of the guidance commands generated by the G&C system [13]-[15]. An effective guidance law can properly assess the trajectory deviation and produce a control force in the necessary direction with the appropriate magnitude. The configuration characteristics and ballistics properties should be taken into consideration when creating the guidance laws, as should the influence of the flight environment.

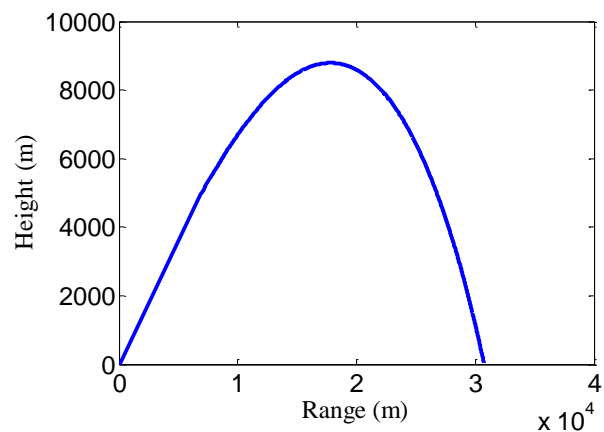


Fig. 3. Trajectory height

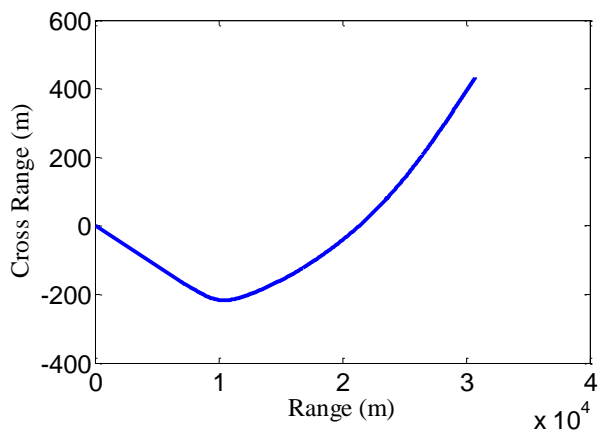


Fig. 4. Cross range

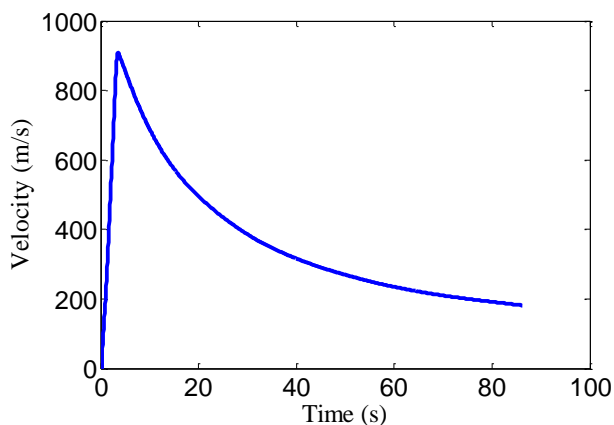


Fig. 5. Total velocity

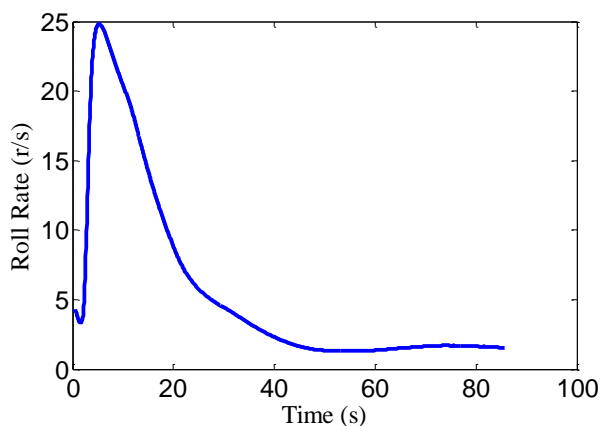


Fig. 6. Roll rate

The trajectory performance for a firing angle of 46° and a range of 31 km is summarized in Figures. 3–6, which show the range, the cross range, the velocity, and the roll rate. From Figure 3, it can be shown that the trajectory is clearly divided into two segments around the trajectory peak, the ascending trajectory and the descending trajectory, and that the trajectory curvature is small. Figure 4 shows the cross range variation that the upwind displacement creates in the powered flight trajectory because of the engine thrust, as well as the downwind displacement that appears in the unpowered flight trajectory as a result of wind. Figure 5 shows that the total velocity reaches a maximum of 910 m/s near the beginning of the trajectory and then decreases progressively. The roll rate is shown in Figure 6, and it can be seen that it also reaches a maximum shortly after launching and eventually remains

consistently around 3r/s after slowing. Considering the above analysis, the challenges to be overcome in the guidance law design can be summarized as follows.

The major challenge is the loss of a line of sight (LOS) to the illuminated target on the ascending trajectory. To successfully collide with the pre-specified target, it is necessary to establish a LOS to the target and the LOS must be directly overhead to be reliable. Furthermore, the horizontal velocity cannot be such that the direct LOS is lost in the ascending segment. Guidance laws that take advantage of the LOS are not currently available.

A second challenge is the trajectory curvature. As the firing angles are always large, the curvature of the trajectory is small, especially at the peak. If a proportional guidance law is used, the proportionality parameter cannot be suitable along the trajectory because the curvature is small, and the shell cannot turn sharply because of the limited control authority. In other words, conventional proportional guidance laws cannot work well with trajectory-corrected rockets with canards.

The other challenge is the lack of control authority. On the one hand, the dynamic pressure is reduced by velocity reduction and the control authority is decreased in the meantime. On the other hand, the trajectory correction is achieved with the accumulation of aerodynamic control, and the control provided by the canards is obviously insufficient to allow the projectile to make sharp turns rapidly. The ability to perform corrections drops as the projectile gets closer to the target. The optimal application of the control authority should be seriously taken into consideration in designing the guidance laws.

Another challenge is the lack of angular feedback. Without an on-board gyroscope or accelerometer, the projectile cannot directly estimate the attitude angles. A new angle feedback method needs to be provided to form a closed G&C loop. The elimination of the Inertial Measurement Unit (IMU) is currently an area of intense study, because flight-qualified gyroscopes that are able to withstand rocket-launch environments are expensive and generate large errors.

The main purpose of this paper is to overcome the above challenges, and to design more suitable guidance laws for trajectory-corrected rockets.

B. Six-Degree-of-Freedom Ballistic Model

To describe the motion of the projectile, three translational and three rotational rigid body degrees of freedom are introduced. This is known as the 6-DOF rigid ballistic model. The translational degrees of freedom are the three components of the mass center position vector [16]. The rotational degrees of freedom are the Euler yaw and pitch angles as well as the roll angle of the shell.

The control signal comes from the deviation between the desired trajectory and the current one. To easily describe the trajectory and guidance law, the coordinate systems shown in Figure 7 are introduced. To describe the relative position between the ideal ballistic curve and the real one, the inertial reference frame $Oxyz$ is introduced. The positive X -axis is in the longitudinal plane and points in the firing direction. The body reference frame $O'x_b y_b z_b$ and the quasi-body reference frame $O'x_q y_q z_q$ are introduced to describe the rotational

motion, and the sequence of rotation from the inertial frame $Oxyz$ is described by the pitch angle φ and yaw angle ψ , as shown in Figure 8. The $O'y_bz_b$ plane of the body reference frame is in the projectile cross section that rotates with the shell. The $O'x_qy_q$ plane of the quasi-body reference frame is fixed in the vertical plane, making it convenient for describing the rotation of the shell.

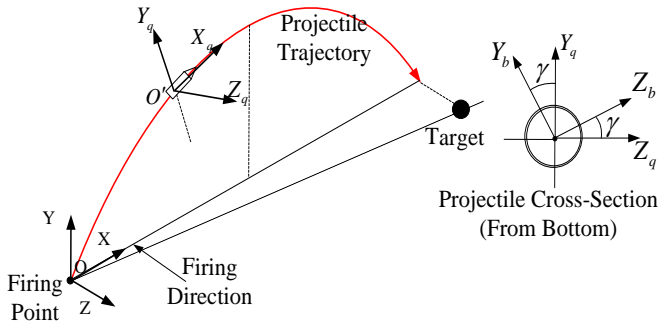


Fig. 7. Coordinate systems

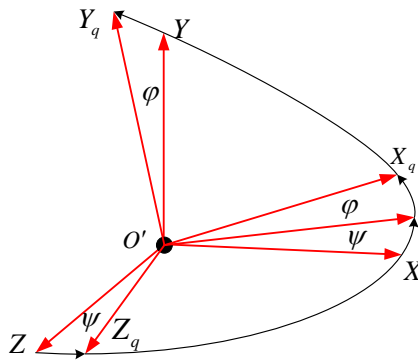


Fig. 8. Coordinate transformations from $Oxyz$ to $O'x_qy_qz_q$

Equations (1–4) represent the translational and rotational kinematic and dynamic equations of motion for the projectile. Both sets of translational equations are expressed in the inertial frame:

$$\begin{bmatrix} \dot{v}_x \\ \dot{v}_y \\ \dot{v}_z \end{bmatrix} + \begin{bmatrix} 0 & \omega_{zq} & -\omega_{yq} \\ \omega_{zq} & 0 & \omega_{zq}t_\psi \\ -\omega_{yq} & -\omega_{zq}t_\psi & 0 \end{bmatrix} \begin{bmatrix} v_x \\ v_y \\ v_z \end{bmatrix} = \frac{1}{m} \begin{bmatrix} F_x \\ F_y \\ F_z \end{bmatrix} + \begin{bmatrix} g_x \\ g_y \\ g_z \end{bmatrix} \quad (1)$$

$$\begin{bmatrix} \dot{x} \\ \dot{y} \\ \dot{z} \end{bmatrix} = \begin{bmatrix} v_x \\ v_y \\ v_z \end{bmatrix} \quad (2)$$

x , y , and z are position vector components of the composite center of mass expressed in the inertial frame. v_x , v_y , and v_z are velocity vector components of the composite center of mass expressed in the inertial frame. F_x , F_y , and F_z are components of the total force expressed in the inertial frame. ω_{xq} , ω_{yq} , and ω_{zq} are components of the angular velocity vector expressed on the axes x_q , y_q , and z_q of the quasi body reference frame.

The two rotational equations are expressed in the

quasi-body reference frame:

$$\begin{bmatrix} J_x \dot{\omega}_{xq} \\ J_y \dot{\omega}_{yq} \\ J_z \dot{\omega}_{zq} \end{bmatrix} = \begin{bmatrix} M_x \\ M_y \\ M_z \end{bmatrix} - \begin{bmatrix} (J_z - J_y) \omega_{yq} \omega_{zq} \\ (J_x - J_z) \omega_{xq} \omega_{zq} \\ (J_y - J_x) \omega_{xq} \omega_{yq} \end{bmatrix} + \begin{bmatrix} 0 \\ -J_z \omega_{zq} \dot{\gamma} \\ -J_z \omega_{zq} \dot{\gamma} \end{bmatrix} \quad (3)$$

$$\begin{bmatrix} \dot{\varphi} \\ \dot{\psi} \\ \dot{\gamma} \end{bmatrix} = \begin{bmatrix} 0 & s_\gamma/c_\psi & c_\gamma/c_\psi \\ 1 & c_\gamma & -s_\gamma \\ 0 & t_\psi s_\gamma & t_\psi c_\gamma \end{bmatrix} \begin{bmatrix} \omega_{xq} \\ \omega_{yq} \\ \omega_{zq} \end{bmatrix} \quad (4)$$

φ , ψ , and γ are yaw, pitch, and roll angle. M_x , M_y , and M_z are components of the total moment expressed on the axes x_q , y_q , and z_q of the quasi body reference frame.

Loads on the composite projectile body are caused by weight and aerodynamic forces. All of the aerodynamic coefficients are acquired by numerical computation. The forces and moments can be presented as follows:

$$\left\{ \begin{array}{l} F_{xq} = -\frac{1}{2} \rho v^2 S C_a \\ F_{yq} = \frac{1}{2} \rho v^2 S C'_n \alpha - \frac{1}{2} \rho v^2 S C'_c \frac{d\dot{\gamma}}{v} \beta \\ \quad - \frac{1}{2} \rho v^2 S C'_c \frac{d\dot{\gamma}}{v} \beta + \frac{1}{2} \rho v^2 S C_{n\delta} (\delta_z c_\gamma + \alpha) \\ F_{zq} = -\frac{1}{2} \rho v^2 S C'_n \beta - \frac{1}{2} \rho v^2 S C'_c \frac{d\dot{\gamma}}{v} \alpha \\ \quad - \frac{1}{2} \rho v^2 S C'_c \frac{d\dot{\gamma}}{v} \alpha - \frac{1}{2} \rho v^2 S C_{n\delta} (-\delta_z s_\gamma + \beta) \\ M_x = -\frac{1}{2} \rho v^2 S L \frac{dp}{v} C_{lp} \\ M_y = \frac{1}{2} \rho v^2 S L m'_z \beta - \frac{1}{2} \rho v^2 S L C_{nr} \frac{Lr}{v} + \frac{1}{2} \rho v^2 S L C_{np} \frac{d\dot{\gamma}}{v} \alpha \\ \quad + \frac{1}{2} \rho v^2 S L C_{np} \frac{d\dot{\gamma}}{v} \alpha + \frac{1}{2} \rho v^2 S L C_{n\delta} (-\delta_z c_\gamma + \beta) \\ M_z = \frac{1}{2} \rho v^2 S L m'_z \alpha - \frac{1}{2} \rho v^2 S L C_{mq} \frac{Lq}{v} - \frac{1}{2} \rho v^2 S L C_{np} \frac{d\dot{\gamma}}{v} \beta \\ \quad - \frac{1}{2} \rho v^2 S L C_{np} \frac{d\dot{\gamma}}{v} \beta + \frac{1}{2} \rho v^2 S L C_{n\delta} (\delta_z s_\gamma + \alpha) \end{array} \right. \quad (5)$$

C_a is the axial force coefficient. C_{np} is the Magnus moment aerodynamic coefficient. C'_n is the normal force derivative coefficient. C'_c is the Magnus force coefficient of the front and aft part. C_{lp} , C_{nr} , and C_{mq} are the roll, yaw, and pitch damping moment coefficients. m'_z is the overturn moment coefficient. α and β are the attack and sideslip angle. δ is the canard deflection angle. ρ is the atmospheric density. v is the total velocity. S and L are the projectile reference area and length. d is the diameter of the projectile.

Note that the force vector $\begin{bmatrix} F_{xq} & F_{yq} & F_{zq} \end{bmatrix}^T$ presents the components of the aerodynamic forces in the quasi-body reference frame, and these should be transformed into the inertial frame for practical application.

The longitudinal and lateral aerodynamic angles of attack are computed as follows:

$$\alpha = -\tan^{-1} \left(\frac{v_{yq}}{v} \right), \beta = \tan^{-1} \left(\frac{v_{zq}}{v} \right) \quad (6)$$

C. Guidance Law Design

On the basis of the rocket configuration and trajectory characteristics, combined with the above analysis, the trajectory can be divided into two segments—the ascending segment and the descending segment, and the guidance laws are designed individually for these two segments. Composite guidance laws are employed using an advanced transversal guidance law in the ascending segment and an advanced proportional guidance law in the descending segment. These processes are introduced in Figure 9 and the details are described in the following sections.

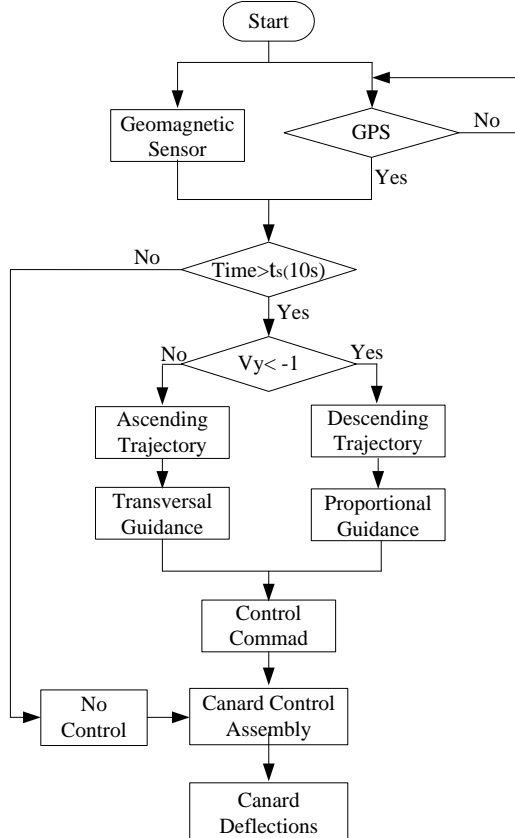


Fig. 9. Guidance law processes

D. The Advanced Transverse Guidance Law in the Ascending Segment

As mentioned previously, because of the limits created by the trajectory curvature and canard properties, a conventional proportional guidance law is not suitable for the ascending segment of the trajectory. Therefore, a transverse guidance law is employed to correct the lateral deviation only, which is contributed to by winds, launch disturbances, parameter perturbations, and aerodynamic deviation. No longitudinal deviation is included. Considering the phenomenon of upwind displacement in the ascending segment and downwind displacement in the descending segment, the terminal lateral deviation is large without control and correction. To diminish the original lateral deviation and avoid wasting the finite control authority, the conventional transverse guidance law should be improved.

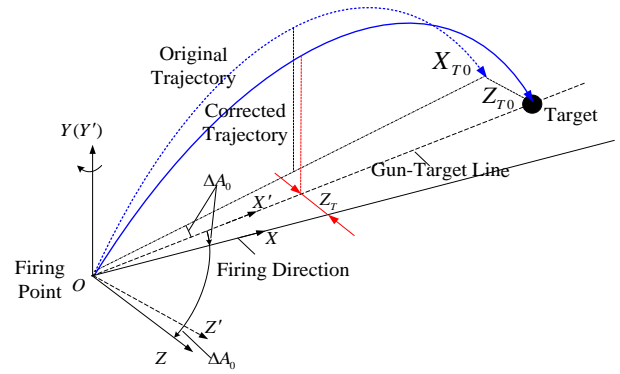


Fig. 10. Advanced transverse guidance law

On the basis of the relative position shown in Figure 10, the lateral deviation in the ascending segment can be denoted by the distance Z_T that the projectile departs from the Gun-Target Line (GTL). For the lateral deviation, the significant influencing factors can be attributed to the lateral position and velocity. If the firing direction is along the GTL without any control conditions, the terminal lateral deviation of the original trajectory is Z_{T0} , as shown in Figure 10. As a consequence, the firing direction should be modified to compensate for the initial lateral deviation. This compensation is achieved by rotating the firing direction with a correction angle ΔA_0 around the $Y(Y')$ -axis at the firing point. The correction angle ΔA_0 is calculated as follows:

$$\Delta A_0 = \arctan \frac{Z_{T0}}{X_{T0}} \quad (7)$$

Under actual field conditions, the correction angle ΔA_0 can be obtained by resolving the trajectory and taking advantage of field measurements of the wind.

With respect to lateral corrections, consequently, the components of the lateral position vector and velocity vector need to be considered. The guidance law for the ascending segment should take the trajectory characteristics into consideration, and an advanced lateral proportional guidance law is employed.

Therefore, the lateral angular deviation can be computed with the equation:

$$\Delta \psi = k_z \cdot Z_T + k_{vz} \cdot V_{zT} \quad (8)$$

where Z_T and V_{zT} are calculated as follows:

$$\begin{cases} Z_T = X \cdot \sin(\Delta A_0) + Z \cdot \cos(\Delta A_0) \\ V_{zT} = V_x \cdot \sin(\Delta A_0) + V_z \cdot \cos(\Delta A_0) \end{cases} \quad (9)$$

Z_T and V_{zT} are the equivalent displacement and velocity of the projectile away from the Gun-Target Line. k_z and k_{vz} are the weight parameters of Z_T and V_{zT} .

As only the lateral deviation is corrected, the initial canard deflection can be obtained as,

$$\delta_0 = \begin{cases} \Delta \psi & 0^\circ < \gamma < 180^\circ \\ -1 \cdot \Delta \psi & 180^\circ < \gamma < 360^\circ \end{cases} \quad (10)$$

To keep the projectile flight stable, the amplitude limiting must be implemented towards the canard deflection. The maximum amplitude of the canard deflection is determined to

be 9° . So the control command, the actual deflection angle δ , can be acquired as:

$$\delta = \begin{cases} 9^\circ & \delta_0 \geq 9^\circ \\ \delta_0 & -9^\circ < \delta_0 < 9^\circ \\ -9^\circ & \delta_0 \leq -9^\circ \end{cases} \quad (11)$$

E. The Advanced Proportional Guidance Law in the Descending Segment

In the descending segment, the trajectory is a smooth curve pointing towards the static target. A proportional guidance law is applied to this segment of the trajectory. Within this guidance law, the lateral and longitudinal deviations are both corrected simultaneously. To fit the trajectory curvature variation, the conventional proportional guidance law must be improved. The advanced guidance law is designed to make use of the relationship between the trajectory slope angle and the LOS angle. The lateral and longitudinal angular deviations are calculated as follows:

$$\begin{aligned} \Delta\varphi &= k_v \cdot V_v \cdot (\dot{q}_v - \dot{\varphi}) \\ \Delta\psi &= k_l \cdot V_l \cdot (\dot{q}_l - \dot{\psi}) \end{aligned} \quad (12)$$

\dot{q}_v and \dot{q}_l are the line of sight angular rate in the lateral and longitudinal planes. k_v and k_l are the lateral and longitudinal proportionality constant. V_v and V_l are the velocities of the projectile away from the Gun-Target Line in the lateral and longitudinal planes.

The above intermediate variables are given by the following equations:

$$\begin{cases} V = \sqrt{V_x^2 + V_y^2 + V_z^2} \\ V_v = V \cdot \cos(\varphi) \\ \dot{q}_v = \frac{V_y \cdot (X - X_T) - V_x \cdot (Y - Y_T)}{(X - X_T)^2 + (Y - Y_T)^2 + (Z - Z_T)^2} \\ V_l = V \cdot \sin(\psi) \\ \dot{q}_l = \frac{V_x \cdot (Z - Z_T) - V_z \cdot (X - X_T)}{(X - X_T)^2 + (Y - Y_T)^2 + (Z - Z_T)^2} \end{cases} \quad (13)$$

The initial canard deflection is provided by the angular deviations in the lateral and longitudinal planes. The equation is given as:

$$\delta_0 = \begin{cases} \sqrt{\Delta\varphi^2 + \Delta\psi^2} & \gamma_c - 90^\circ < \gamma < \gamma_c + 90^\circ \in [0^\circ, 360^\circ] \\ -1 \cdot \sqrt{\Delta\varphi^2 + \Delta\psi^2} & \gamma_c + 90^\circ < \gamma < \gamma_c + 270^\circ \in [0^\circ, 360^\circ] \end{cases} \quad (14)$$

$$\gamma_c = \arctan \frac{\Delta\varphi}{\Delta\psi} \quad 0^\circ < \gamma_c < 360^\circ$$

where γ_c is determined from the relationship between the lateral and longitudinal angular deviations, and is illustrated in Figure 11.

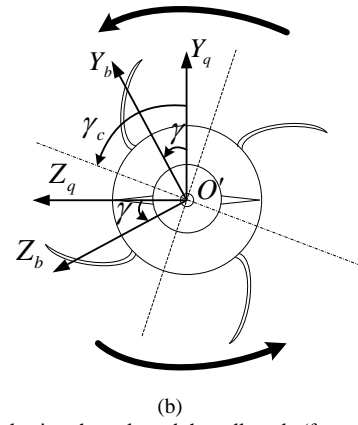
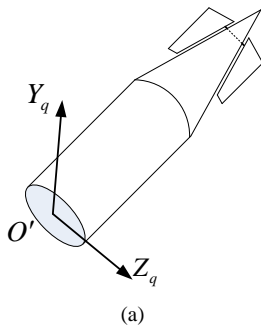


Fig. 11. The control azimuth angle and the roll angle (from a warhead)

In addition, stability of flight should be ensured and amplitude limiting is encouraged. The actual canard deflection is given as equation 11.

IV. SIMULATION ANALYSIS

A. Hardware Loop Simulation

In this section, a loop simulation of the hardware is presented to demonstrate the effectiveness of the guidance law [17, 18]. The actuator characteristics are also considered. Testing the hardware in a loop simulation has three key purposes: 1) verifying the feasibility of the guidance law design, 2) testing the effectiveness of the guidance law, and 3) acquiring the transform function to be introduced into the closed control loop to improve the control parameters of the guidance law.

Scheme Design

The simulation system consists of a combination of G&C equipment, including a projectile-borne computer, a canard actuator with guidance law algorithms, and a simulation computer to form the closed simulation loop.

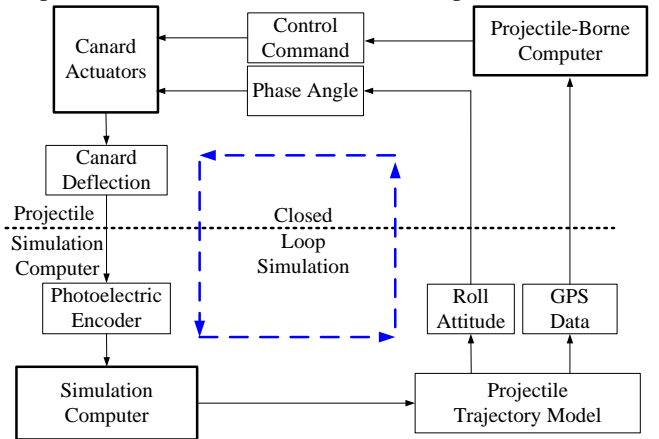


Fig. 12. Block diagram of the hardware assumed in the loop simulation system

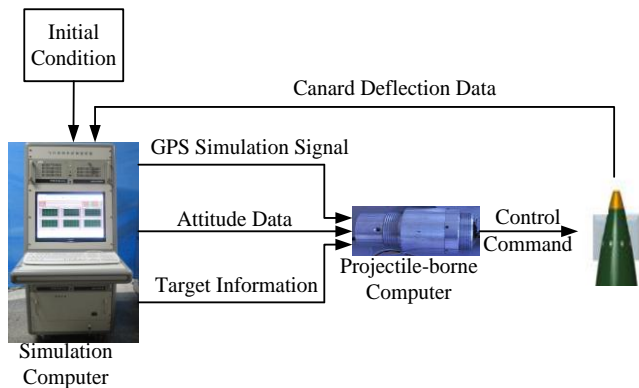


Fig. 13. A physical photo of the hardware in the loop simulation system

In the simulation experiment, the simulation computer resolves the trajectory information in accordance with the six-degree-of-freedom ballistic model with Matlab/Simulink. The simulation computer uses the ballistic model to provide the simulated GPS data, the projectile position and velocity, and the simulated roll attitude to produce a 100-Hz navigation solution. The navigation data are then transmitted to the projectile-borne computer. This computer combines navigation data with the pre-specified target location to measure the deviation angles between the actual flight path and the ideal one. The guidance law is employed to resolve the trajectory deviations and to produce the guidance command, also in 100 Hz. The control command is computed by the algorithm and transmitted to the canard actuator to execute a canard deflection angle δ at a specific roll angle, the control roll angle γ_c . At the same time, the real deflection angle is measured by the photoelectric encoder to analyze the final trajectory and control signal error. As the angle is passed to the simulation computer to compute the new trajectory, a closed loop simulation is achieved. A block diagram of the scheme design is shown in Figure 12 and a physical photo is shown in Figure 13.

Initial Conditions

To resolve the trajectory, the initial conditions are given, including initial firing data, environment information, and measurement errors, in Tables I and II. The firing angle and azimuth angle can be computed from the relation between the positions of the firing point and aim-point. During flight, the GPS simulation data and roll angles are generated with noise. The wind distribution is obtained from field measurements. The wind velocities and directions are shown in Table II.

Prior to firing, the projectiles are initialized with aim-point information that will be utilized in the guidance law algorithm during the flight. The aim-point coordinates for the simulation are (33180, 6, 205) in the inertial reference frame.

TABLE I
SIMULATION CONDITIONS

Characteristics	Value
Firing angle	43°
Exit velocity	38m/s
Exit Roll Rate	3r/s
Wind	Table. II
GPS velocity noise	0.3m/s
GPS position noise	10m/s
Roll angle error	3°(random)

TABLE II
WIND DISTRIBUTION

Height (m)	Velocity (m/s)	Direction (°)	Height (m)	Velocity (m/s)	Direction (°)
0	3.5	212	3600	7.1	294
100	5.8	217	3800	7.2	275
200	5.9	218	4000	6.7	268
300	7.5	215	4400	4.3	302
400	8.9	212	4800	7.4	307
500	10.4	209	5000	8.4	309
600	10.2	210	5400	9.8	312
700	9.5	211	5800	10.6	314
800	8.9	213	6000	10.6	311
900	8.2	219	6400	12.3	317
1000	7.4	232	6800	12.7	315
1100	6.6	246	7000	13.1	320
1200	5.8	260	7400	14.1	325
1300	5.3	276	7800	15	323
1400	4.9	292	8000	15.1	322
1500	4.5	308	8400	15.6	321
1600	4.2	316	8800	16.3	319
1700	3.9	319	9000	16.5	317
1800	3.6	322	9400	17.7	314
1900	3.6	324	9800	17.9	312
2000	4	324	10000	17.6	312
2200	4.9	324	11000	18.3	317
2400	5.1	300	12000	24.3	318
2600	5	279	13000	23.8	317
2800	4	280	14000	19.1	308
3000	4.1	286	15000	17	305
3200	5.7	298			
3400	6.6	299			

Simulation Results

The simulation results are shown in Figures. 14–21. Figures. 14-15 compare the uncontrolled and controlled flight paths in terms of the trajectory height and cross range. If the projectile is not corrected during the flight, the aim-point coordinate should be (32507, 6, 738), with a terminal miss of lateral deviation 533 m and longitudinal deviation -673 m. Figure 16 and Figure 17 show the variation in the deviations corresponds with the trajectory correction. From the figures, it can be seen that the trajectory deviations have obviously been corrected. The actual aim-point (33181, 6, 201) is close to the desired aim-point (33180, 6, 205) with a terminal miss of lateral deviation 4 m and longitudinal deviation 1 m. It is therefore seen that the guidance law can work well to reduce the trajectory deviation and steer the projectile to the desired aim-point.

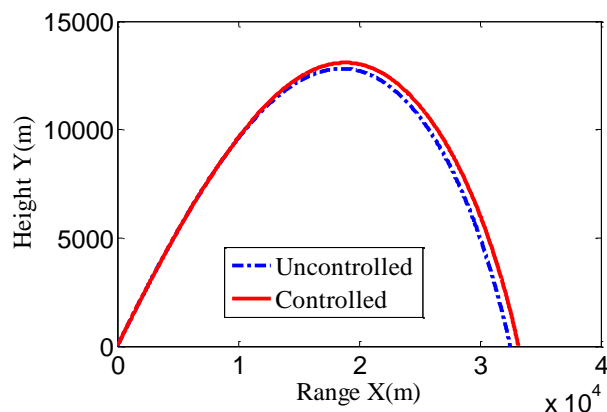


Fig. 14. Trajectory height

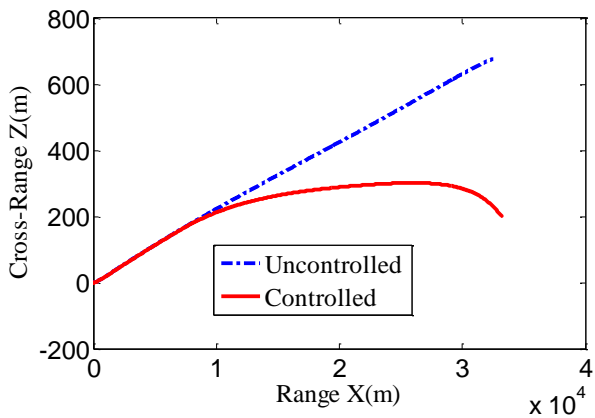


Fig. 15. Trajectory cross range

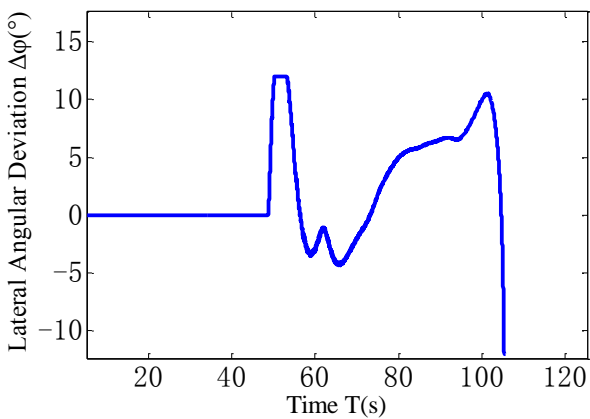


Fig. 16. Lateral angular deviations

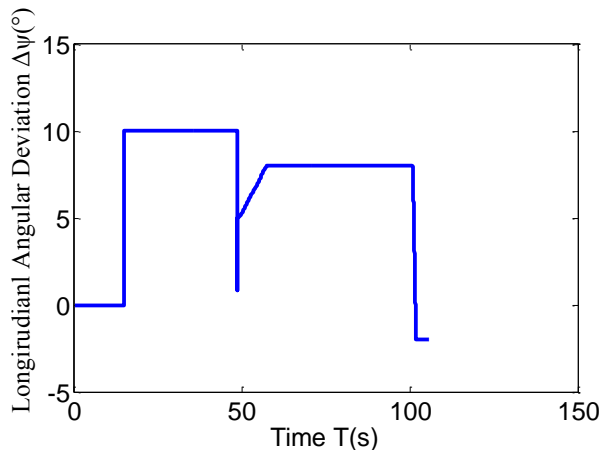


Fig. 17. Longitudinal angular deviations

Figures. 18-19 illustrate the results for the hardware in the loop simulation. The control commands of the onboard computer are aligned with the commands of the simulation computer. The canard deflection can follow the control command well with a small error of 0.5 °, as can be seen in Figures. 20-21. The results show that the guidance laws are both feasible and effective.

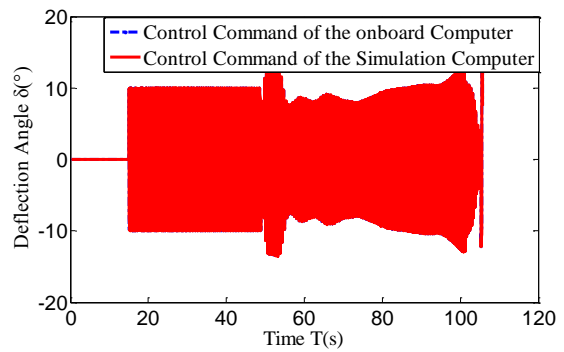


Fig. 18. Results of the control command

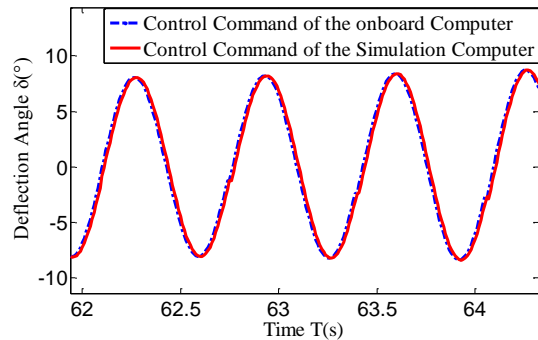


Fig. 19. Magnification of the results of the control command

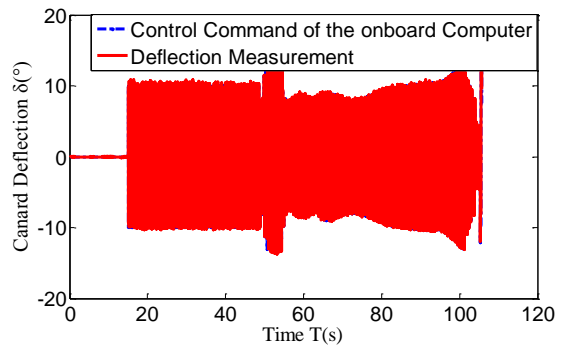


Fig. 20. Results of the canard deflection

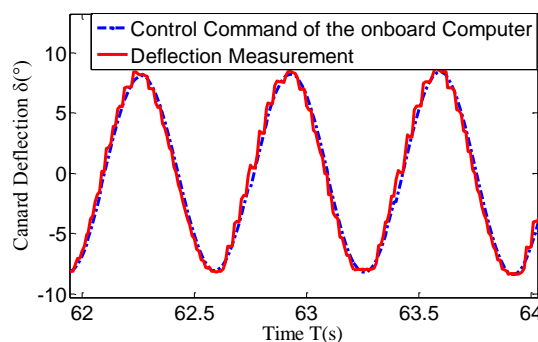


Fig. 21. Magnification of the results of the canard deflection

Monte Carlo Simulations

A Monte Carlo method was also applied to demonstrate the performance of the guidance law with variable disturbances and errors. The dispersion always results from a combination of initial launching point errors, velocity variation, engine thrust variation, aerodynamic disturbances, GPS errors, and wind disturbances that cause the projectile trajectory to deviate from the expected trajectory, as described in Table III.

TABLE III
DEVIATIONS

Characteristics		Deviation Value
Initial	Firing angle	1.0°(3σ)
Disturbance	Launch Azimuth	0.5°(3σ)
	Projectile Mass	0.4Kg(3σ)
Mass Deviation	Polar moment of inertia	2%(3σ)
	Equator moment of inertia	2%(3σ)
	Axial Force Coefficient	2%
Aerodynamic coefficient	Normal Force Coefficient	3%
	Yawing Force Coefficient	5%
	Roll Moments	10%
	Pitching Moments	10%
Wind	Yawing Moments	10%
		Table. II
	GPS velocity noise	0.3m/s
	GPS position noise	10m/s

Figures. 22-23 compare the impact point results at a range of 31 km for the uncontrolled and controlled dispersion cases with a Monte Carlo simulation analog target. After statistical analysis, the guidance law improves the Circle Error Probable (CEP) from 446.3 m (uncontrolled) to 4.1 m (controlled). Note that the CEP is calculated around the mean impact value for each case. These results prove that the advanced guidance law can significantly improve accuracy.

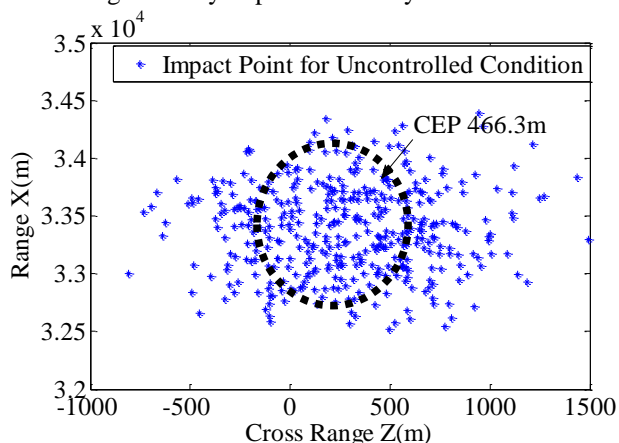


Fig. 22. Monte Carlo dispersion and CEP under uncontrolled conditions

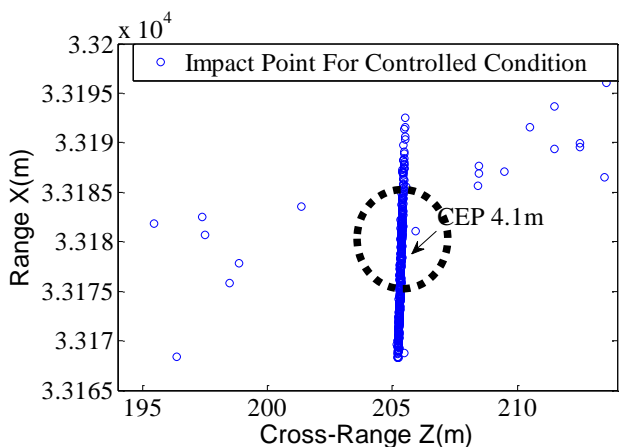


Fig. 23. Monte Carlo dispersion and CEP under controlled conditions

V. CONCLUSION

This research shows that trajectory-corrected rockets with a pair of canards under single-channel control can be effectively controlled using only GPS and geomagnetic

measurements. It also shows that the advanced guidance law presented is suitable and can achieve satisfactory precision. With the hardware in the loop simulation, the angle feedback of the actuator action agrees well with the control command of the projectile-borne computer, both in the trend and value. The results of the Monte Carlo method simulation verify that the guidance law presented is sufficiently effective for the design to be suitable for future research.

REFERENCES

- [1] F. Fresconi, "Guidance and Control of a Projectile with Reduced Sensor and Actuator Requirements," *Journal of Guidance, Control, and Dynamics*, Vol. 34, No. 6, 2011, pp. 1757-1766.
- [2] L. H. Johnson, "Precision Guidance Kit", *56th Annual Fuze Conference*, Baltimore, MD., 2012.
- [3] P. Myrick, "Affordable Precision Artillery Precision Guidance Kit (PGK)," *8th Annual Future Artillery Conference*, London, 2010.
- [4] Y. Wang, W. Song, Q. Guo, X. Song, and G. Wang, "Correction mechanism analysis for a class of spin-stabilized projectile with fixed canards," *Engineering Letters*, Vol. 23, No. 4, 2015, pp. 269-276.
- [5] D. A. Bittle, G. A. Hall, R. W. Nourse, "Roll isolation bearing design and testing for low cost precision kill missile system," *AIAA Defense and Civil Space Programs Conference and Exhibit*, Huntsville, AL, 1998, pp. 52-61.
- [6] A. E. Gamble, P. N. Jenkins, "Low Cost Guidance for the Multiple Launch Rocket System (MLRS) Artillery Rocket," *Aerospace and Electronic Systems Magazine, IEEE*, Vol. 16, No. 1, 2001, pp. 33-39.
- [7] N. Barbour, G. Schmidt, "Inertial sensor technology trends," *Sensors Journal*, Vol. 1, Issue 4, 2001, pp. 332-339.
- [8] M. Gao, Y. Zhang, S. Yang, and D. Fang, "Trajectory correction capability modeling of the guided projectiles with impulse thrusters," *Engineering Letters*, Vol. 24, No. 1, 2016, pp. 11-18.
- [9] M. F. Costello, "Potential Field Artillery Projectile Improvement Using Movable Canards," US: Aberdeen Proving Ground, US Army Research Laboratory, ARL-TR-1344, 1997.
- [10] M. F. Costello, "Range Extension and Accuracy Improvement of an Advanced Projectile Using Canard Controlled," *AIAA Atmospheric Flight Mechanics Conference*, Baltimore, MD., 1995, pp. 324-331.
- [11] D. Ollerenshaw, M. F. Costello, "Model Predictive Control of a Direct Fire Projectile Equipped with Canards," *AIAA Atmospheric Flight Mechanics Conference*, San Francisco, CA, 2005.
- [12] Rogers J., Costello M., Harkins T., and Hamaoui M., "Effective Use of Magnetometer Feedback for Smart Projectile Applications," *Navigation*, Vol. 58, No. 3, 2011, pp. 203-219.
- [13] F. Fresconi, P. Plostins, "Control Mechanism Strategies for Spin-Stabilized Projectiles," *Journal of Aerospace Engineering*, Vol. 224, No. 9, 2010, pp. 979-991.
- [14] D. Ollerenshaw, Mark Costello, "Simplified projectile swerve solution for general control inputs," *Journal of Guidance, Control, and Dynamics*, Vol. 31, No. 5, 2008, pp. 1259-1265
- [15] S. Theodoulis, V. Gassmann, P. Wernert, "Guidance and control design for a class of spin-stabilized fin-controlled projectiles," *Journal of Guidance, Control and Dynamics*, Vol. 36, No. 2, 2013, pp. 517-531.
- [16] M. F. Costello, "Modeling and simulation of a differential roll projectile," *AIAA Modeling and Simulation Technologies Conference*, Boston, MA, 1998, pp. 490-499.
- [17] J. A. Ray, G. A. Larson, J. E. Terry, "Hardware-in-the-loop support of the Longbow/HELLFIRE modular missile systems preplanned product improvement program," *Technologies for Synthetic Environments: Hardware-in-the-loop Testing VI*, Orlando, Florida, April 2001, pp. 519-527.
- [18] J. Zhang, G. Wang, Y. Hao, "The investigation of aerodynamic characteristics for two-dimensional trajectory correction projectile canard rudder device," *Journal of Projectiles, Rockets, Missiles, and Guidance*, Vol. 33, No. 2, 2013, pp. 88-91. (in Chinese)